Hindawi
Journal of Chemistry
Volume 2018, Article ID 1461673, 9 pages
https://doi.org/10.1155/2018/1461673

*Research Article*

# The Organic Pollutant Characteristics of Lurgi Coal Gasification Wastewater before and after Ozonation

**Chunrong Wang, Qi Zhang, Longxin Jiang, and Zhifei Hou**

*School of Chemical and Environmental Engineering, China University of Mining and Technology (Beijing), Beijing 100083, China*

Correspondence should be addressed to Chunrong Wang; wcrzgz@126.com

Received 5 December 2017; Revised 17 May 2018; Accepted 5 June 2018; Published 5 July 2018

Academic Editor: Sabrina Copelli



The effluent of distilled and extracted Lurgi coal gasification wastewater has been found to have low biodegradability and high toxicity, which inhibits further biodegradation. However, ozonation enhances the biodegradability and reduces the toxicity of this effluent, enabling further biological treatment and increased removal of organic materials. In this study, the dissolved organic matters in Lurgi coal gasification wastewater were isolated into six classes by resin adsorbents, after which TOC, $UV_{254}$, UV-Vis, and 3D EEM were employed to quantitatively and qualitatively analyze organic materials in each part of the fractionated samples. The HoA and HiN fraction accounted for large amounts of the Lurgi coal gasification wastewater, and their TOC values were about 380.21 $mg{\cdot}L^{-1}$ and 646.84 $mg{\cdot}L^{-1}$, respectively. After ozonation, the TOC removal rates of HoA and HiN reached 42.85% and 67.13%, respectively. The $UV_{254}$ of HoA was basically stable before and after ozonation, while that of HiN increased continuously because a portion of the humic macromolecular organic materials in HoA was oxidized to HiN. Additionally, UV-Vis analysis revealed that the larger molecular organics of HoA were oxidized during ozonation, resulting in high biodegradability. Finally, the 3D EEM spectra indicated that the macromolecular organics were oxidized to smaller molecules with the degradation of soluble microbial by-products.

## 1. Introduction

Coal exploitation and consumption have been growing rapidly and causing serious environmental pollution; accordingly, there is a demand for efficient, safe, and clean utilization of coal [1, 2]. Therefore, a new type of coal chemical engineering technology is needed to optimize the use of coal. As one of the most widely used coal gasification technologies, Lurgi gasification generates various contaminants during the cleaning and washing of gas [3]. After ammonia distillation and dephenolization, Lurgi coal gasification wastewater (LCGW) is still a complex industrial wastewater containing high concentrations of organic matter, ammonia, and prussiate [4], resulting in unsatisfactory effluent quality after anaerobic-anoxic-oxic (A-A-O) process and sequencing batch reactor (SBR) biological treatment process [5].

Most studies of gasification wastewater quality conducted in recent years have focused on its quality. The LCGW treatment process has been widely investigated, but these studies have investigated the COD, TOC, $BOD_5$, and other simple indicators, which showed that gasification wastewater was characterized by high levels of organic pollutants, low biodegradability, and high toxicity [6–8]. Moreover, previous studies have demonstrated that after ammonia distillation and dephenolization, the LCGW still contained phenolics, polycyclic aromatic hydrocarbons, and nitrogen heterocyclic compounds [9–11]. Because of the high amounts of common organic pollutants, the biological treatment of LCGW led to poor biodegradation. However, few studies have included systematic analyses of wastewater qualities of LCGW. Moreover, identification of methods for the transformation of organic pollutants during the treatment of LCGW is urgently needed.

Before biological treatment of LCGW, ammonia distillation and dephenolization were applied to remove the organic pollutants. Because of the limited removal efficiency of ammonia distillation and dephenolization, most organics were removed by biological treatments, such as hydrolyzation acidification, activated sludge processes, sequencing batch reactor (SBR), anoxic-oxic (A/O) processes, and anaerobic-anoxic-oxic ($A^2/O$) processes [12].

However, the main characteristics of the effluents after biological treatment were as follows: 100–200 $mg{\cdot}L^{-1}$ of COD, 0.01–0.08 of $BOD_5$/COD ratio (B/C), 40–70 $mg{\cdot}L^{-1}$ of total nitrogen (TN), 10–20 $mg{\cdot}L^{-1}$ of $NH_4^+$-N, and 90–120 $mg{\cdot}L^{-1}$ of TOC [13–16]. Moreover, most studies only used simple indexes to express the characteristics of LCGW, and none have analyzed the effects of qualities on treatment process or the transformation of organic compounds during treatment. According to the national LCGW discharge policy of China, especially the requirement of zero liquid discharge, more measures for the advanced biological treatment of LCGW effluent are needed [17]. Because the effluent after ammonia distillation and dephenolization has low biodegradability and high toxicity, ozonation is commonly applied to enhance the removal rate of organic materials because it improves biodegradability, enabling further biological treatment. Nevertheless, when compared with the removal rate, the transformation of organics during ozonation has received less attention. Moreover, the analysis of raw LCGW quality was difficult because of the complexity characteristic [18].

Therefore, this study was conducted to investigate the characteristics of LCGW after ammonia distillation, dephenolization, and organics transformation and to investigate the effects of organics on ozonation. Fractionation of the LCGW after ammonia distillation and dephenolization was conducted using resin adsorption, after which the dissolved organic carbon (DOC), $UV_{254}$, UV-Vis, and EEM were used to quantify organic matter in each part of the fractionated samples. Following ozonation, DOM was analyzed in the solution, and the effects of organics on ozonation were further examined. The results presented herein will serve as a reference for further engineering application, guiding the commission and normal operation of future treatment facilities.

## 2. Materials and Methods

*2.1. Wastewater Samples.* Lurgi coal gasification wastewater samples were obtained from the effluent of ammonia stripping and phenolic solvent extraction processes in a Lurgi coal gasification wastewater treatment plant (Henan Coal Chemical Industry Group Co., Ltd.). The raw water was filtered through a 0.45 $\mu$m cellulose membrane (PES) to obtain dissolved organic matters (DOMs). All experimental data were analyzed using SPSS 17.0. The data were analyzed as the means of three replicates, and differences were considered significant at a $p$ value < 0.05. The characteristics of the coal gasification wastewater discharge are listed in Table 1.

Table 1: Main physical and chemical properties of LCGW discharge in this plant.

| Parameter | Concentration | Unit |
|---|---|---|
| pH | $8.0 \pm 0.16$ | |
| COD | $4066.67 \pm 200$ | $mg{\cdot}L^{-1}$ |
| TOC | $1214 \pm 50$ | $mg{\cdot}L^{-1}$ |
| $BOD_5$ | $419 \pm 10$ | $mg{\cdot}L^{-1}$ |
| $NH_4^+$-H | $300 \pm 20$ | $mg{\cdot}L^{-1}$ |
| $CN^-$ | $0.009 \pm 0.001$ | $mg{\cdot}L^{-1}$ |
| Oil | $58.34 \pm 3$ | $mg{\cdot}L^{-1}$ |
| Benzopyrene | $0.00082 \pm 0.00003$ | $mg{\cdot}L^{-1}$ |

*2.2. Ozonation Equipment.* The ozonation equipment is shown in Figure 1. Ozonation was conducted at room temperature in a semicontinuous model reactor with an effective volume of 1.5 L. The optimum reaction time was selected based on Figure 1S, while the optimum pH was based on Figure 2S. Ozone gas was generated using a VMUS-1SE laboratory ozone generator (AZCO Industries LTD, Canada) rated at 5.7 mg $O_3\,L^{-1}$ (based on Figures 3S and 4S). In a typical experiment, 1 L of LCGW was added into the borosilicate glass reactor (1000 mm tall and 50 mm in diameter); after which, ozone was continuously fed to the wastewater through a microporous titanium plate at the bottom of the reactor to obtain gas bubbles at the same time. The input gas pressure was 0.04 MPa, and the gas flow rate was 3 L $min^{-1}$. The excess ozone in the outlet gas was absorbed by 5% $Na_2S_2O_3$ solution. Total organic carbon (TOC), $UV_{254}$, UV-Vis, and EEM were determined at different times.

*2.3. Analytical Methods.* The concentration of ozone in in-gas and off-gas was measured using an ozone analyzer (ZX-01, China). Gaseous ozone in off-gas was continuously introduced to the ozone analyzer, while the concentration of ozone dissolved in the aqueous phase was determined using the indigo method. Before the test of resin fractionation, the resins (Amberlite XAD-8 nonionic resin, Dowex 50WX2 $H^+$ cation exchange resin, and Amberlite IRA-958 ($Cl^-$) anion exchange resin) were Soxhlet-extracted with methanol for 24 h and then rinsed with acid-base solutions and Milli-Q water (Supplementary Material for details). After pretreatment of resins, DOM fractionation via the adsorbent resin method was employed to separate the dissolved organic matter into six groups: hydrophobic acid (HoA), hydrophobic neutral (HoN), hydrophobic base (HoB), hydrophilic acid (HiA), hydrophilic neutral (HiN), and hydrophilic base (HiB) [19]. In addition, the TOC in the water was determined using a TOC analyzer (Shimadzu, TOC-VCPN, Japan) after filtration through 0.45 $\mu$m cellulose membrane. The $UV_{254}$ in each degraded solution was monitored by UV-visible spectroscopy (Hach, DR5000, USA). Fluorescence was determined using a HITACHIF-7000 spectrofluorometer. The EEM was conducted using a 1500 W xenon lamp, PMT voltage of 500 V, excitation and emission of 200 to 450 nm and 220 to 600 nm, respectively, a scanning speed of 1200 $nm{\cdot}min^{-1}$, and the slit widths of 5 nm. Before analysis, the Raman scattering and Rayleigh scatter effects were removed.

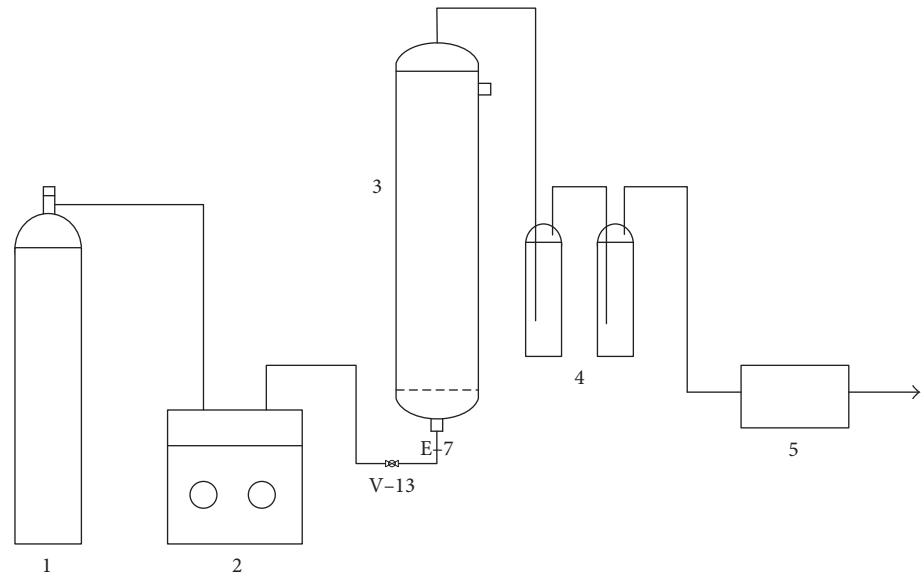


Figure 1: Schematic diagram of ozonation experiment. 1: oxygen cylinder, 2: ozone generator, 3: sample tap, 4: KI trap, and 5: ozone absorber.

## 3. Results and Discussion

*3.1. Distribution Characteristics for TOC before and after Ozonation.* The results revealed that TOC was present in each of the fractions; therefore, further analysis was conducted to determine the distribution of organic carbon in LCGW. The phenols and their derivatives in the LCGW effluent accounted for 53.30% of the total COD, which reached 2712.36 mg·L$^{-1}$. Furthermore, recalcitrant organic compounds such as pyridine, indole, quinolone, biphenyl, and other aromatic derivatives accounted for a high proportion of TOC in traditional LCGW. Ozonation effectively oxidized organic compounds with unsaturated bonds, especially in LCGW, because of its dipole structure. The TOC concentrations of the six separated components in the LCGW before and after ozonation are shown in Figure 2.

As shown in Figure 2, the main components of DOM in the current study were HoA and HiN with a concentration of 380.21 mg·L$^{-1}$ and 646.84 mg·L$^{-1}$, respectively. The concentration of TOC decreased from 1214.51 mg·L$^{-1}$ to 537.31 mg·L$^{-1}$ after ozonation with a removal rate of 55.76%. The removal rates of HoA in 60 min and 120 min were 21.23% and 42.85%, respectively, while the TOC of HoB remained stable during the process. Although the removal rate of HoN reached as high as 95.38% in 120 min, it had little influence on total TOC because its initial concentration was only 5.40 mg·L$^{-1}$. Moreover, HiA and HiB reached a TOC removal rate of 56.00% and 50.28%, respectively, while the rate of HiN reached 56.01% in 60 min and 67.13% in 120 min. Taking together, these findings indicated that ozonation mainly showed a significant effect on HoA and HiN of TOC removal, while its effects on other components were lower.

*3.2. Distribution Characteristics for $UV_{254}$ before and after Ozonation.* The $UV_{254}$ value was measured using a colorimetric dish as the carrier for solutions. To accomplish this, the absorbance of the sample at 254 nm was measured in an ultraviolet spectrophotometer. The $UV_{254}$ values can represent the concentration of TOC qualitatively to some extent. The polycyclic aromatic hydrocarbons and nitrogen heterocyclic compounds present in effluent are still difficult to degrade by biochemical treatment, despite the low level of phenols in the LCGW and good performance of biochemical technology at removing the phenols remaining in the effluent. The $UV_{254}$ value can also be used to measure the degree of humification as most DOMs in natural waters are humic substances. The ratio of $UV_{254}$ of the components in total DOM values is shown in Figure 3.

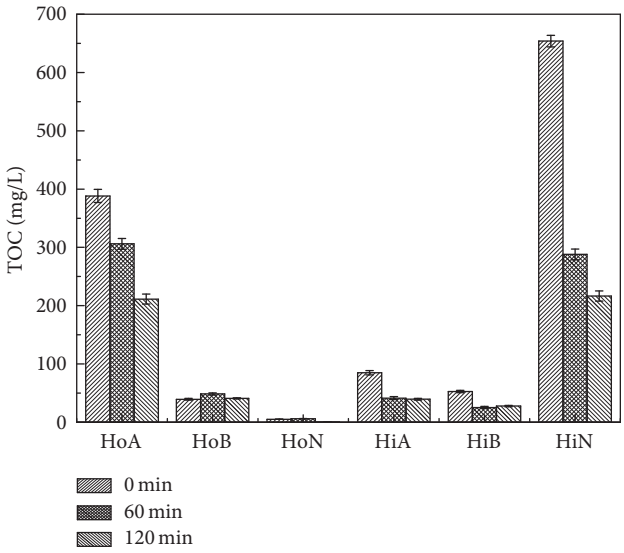


Figure 2: TOC of the components when the reaction time was 0 min, 60 min, and 120 min.

The main components of DOM were HoA and HiN, which accounted for 31.30% and 53.26% of the total, while

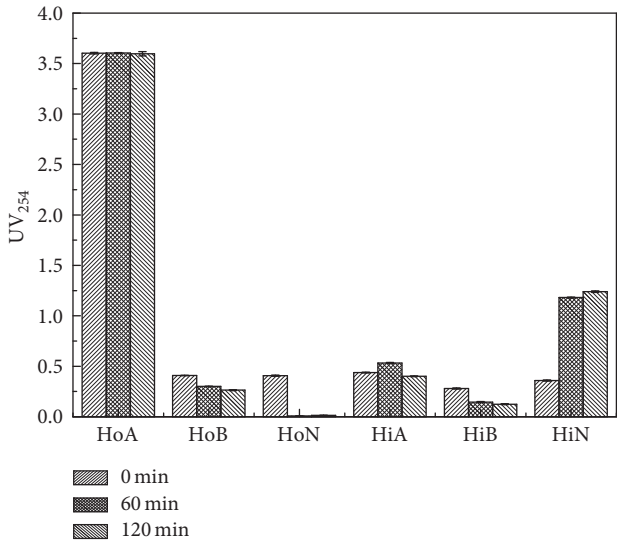


Figure 3: $UV_{254}$ of the components when the reaction time is 0 min, 60 min, and 120 min.

HiA, HiB, HoB, and HoN accounted for only 7.20%, 4.46%, 3.33%, and 0.44% of the total, respectively. Among these, HoA had the highest ratio of $UV_{254}$, accounting for 65.66%, while the $UV_{254}$ values in HiA, HiB, HiN, HoB, and HoN were 8.02%, 5.15%, 6.44%, 7.40%, and 7.33%, respectively, demonstrating that there were large amounts of aromatic compounds in HoA. These findings also indirectly explained the high TOC values in HoA.

Ozonation leads to different degrees of decrease for most components, with the highest removal rate being observed for HoN and the lowest for HiN. However, the $UV_{254}$ values of HoA remained basically unchanged and that of HiN increased continuously. Based on previous studies, the reason for the increase in the $UV_{254}$ value can be explained as follows: First, C=O was generated during ozonation because the hydroxy group was oxidized or the benzene ring was destroyed [20–22]. Second, the unsaturated group in the hydrophobic substances will be destroyed by ozonation, resulting in the material structure of HoA changing and the hydrophobic substances being transferred to other kinds of materials, leading to oxidation of the humic macromolecule organic materials in HoA generating HiN.

*3.3. UV-Vis Spectral Analysis of DOM in LCGW before and after Ozonation.* UV-Vis spectra analysis can effectively be used for determination of specific functional groups in water samples and further indication of the characteristics of DOM. However, the number of chromophoric groups that generated absorption peaks in the spectrum was so large that it was difficult to identify groups clearly. Figure 4 shows the spectrogram of separated components before and after ozonation.

As shown in Figure 4, similar waveforms appeared in the spectrum with few distinct peaks and troughs. In addition, many peaks overlapped, which may be explained by the presence of humic substances. As shown in Figure 4(a), the maximum absorbance of each component except HoN was about 220 nm, while every component except HoA

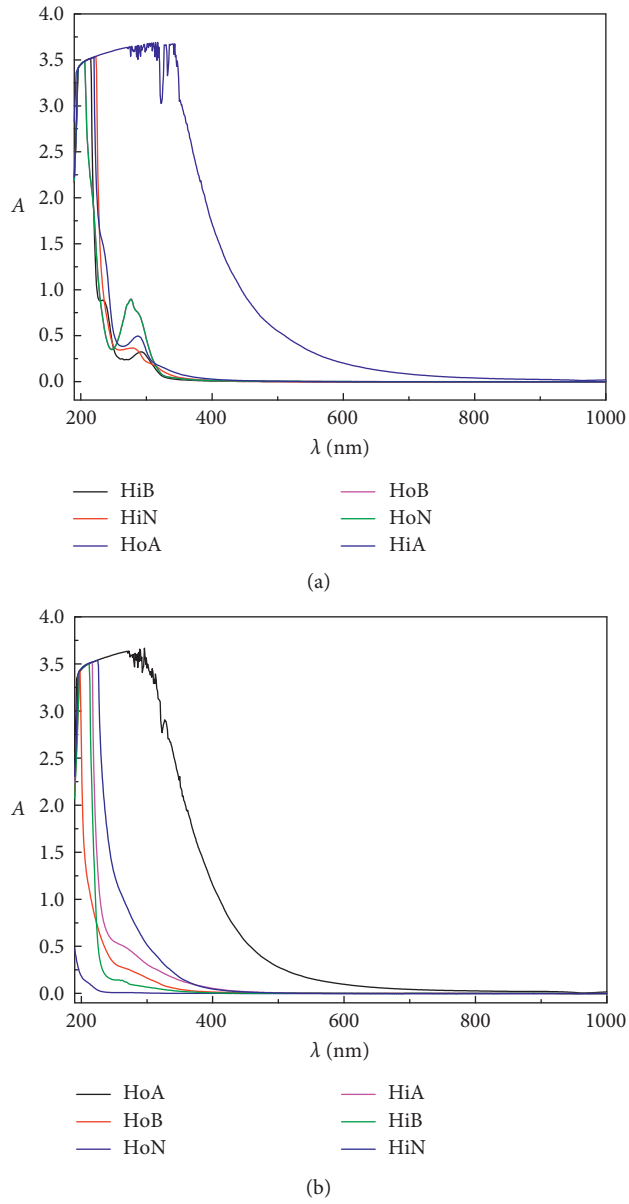


Figure 4: Ultraviolet-visible absorption spectroscopy of DOM components when the reaction time is 0 min (a) and 120 min (b).

generated a distinct absorbance peak at 270–290 nm. As shown in Figure 4(b), the absorbance at 270–290 nm disappeared after ozonation with corresponding R absorption band. This was a result of lone pairs of electrons on the heteroatoms connected with double bonds being transferred to the $\pi^*$ antibonding orbital and indicated that double-bond heteroatoms were all oxidized during ozonation.

The spectrum is unable to provide much information about the properties of DOM. Moreover, the degree of humification maintains at a high level, and unsaturated organic components are concentrated in the ultraviolet area. The complexity of organic components also leads to the overlap of absorption peaks; therefore, more detailed information about components is difficult to achieve. $E_{254}/E_{365}$, $E_{300}/E_{400}$, and SR values of each component are shown in Table 2.

Table 2: UV-visible spectral parameters of the DOM components.

| 0 min | $UV_{254}$ | $E_{254}/E_{365}$ | $E_{300}/E_{400}$ |
|---|---|---|---|
| HoA | 3.609 | 1.34 | 2.10 |
| HoB | 0.407 | 15.65 | 35.77 |
| HoN | 0.403 | 17.52 | 42 |
| HiA | 0.441 | 7.47 | 11.82 |
| HiB | 0.283 | 17.69 | 39.86 |
| HiN | 0.354 | 11.42 | 16.69 |
| 120 min | $UV_{254}$ | $E_{254}/E_{365}$ | $E_{300}/E_{400}$ |
| HoA | 3.609 | 3.42 | 3.925 |
| HoB | 0.267 | 5.93 | 4.69 |
| HoN | 0.011 | 5.5 | 3 |
| HiA | 0.398 | 4.85 | 5.78 |
| HiB | 0.121 | 9.64 | 12.2 |
| HiN | 1.245 | 6.96 | 6.53 |

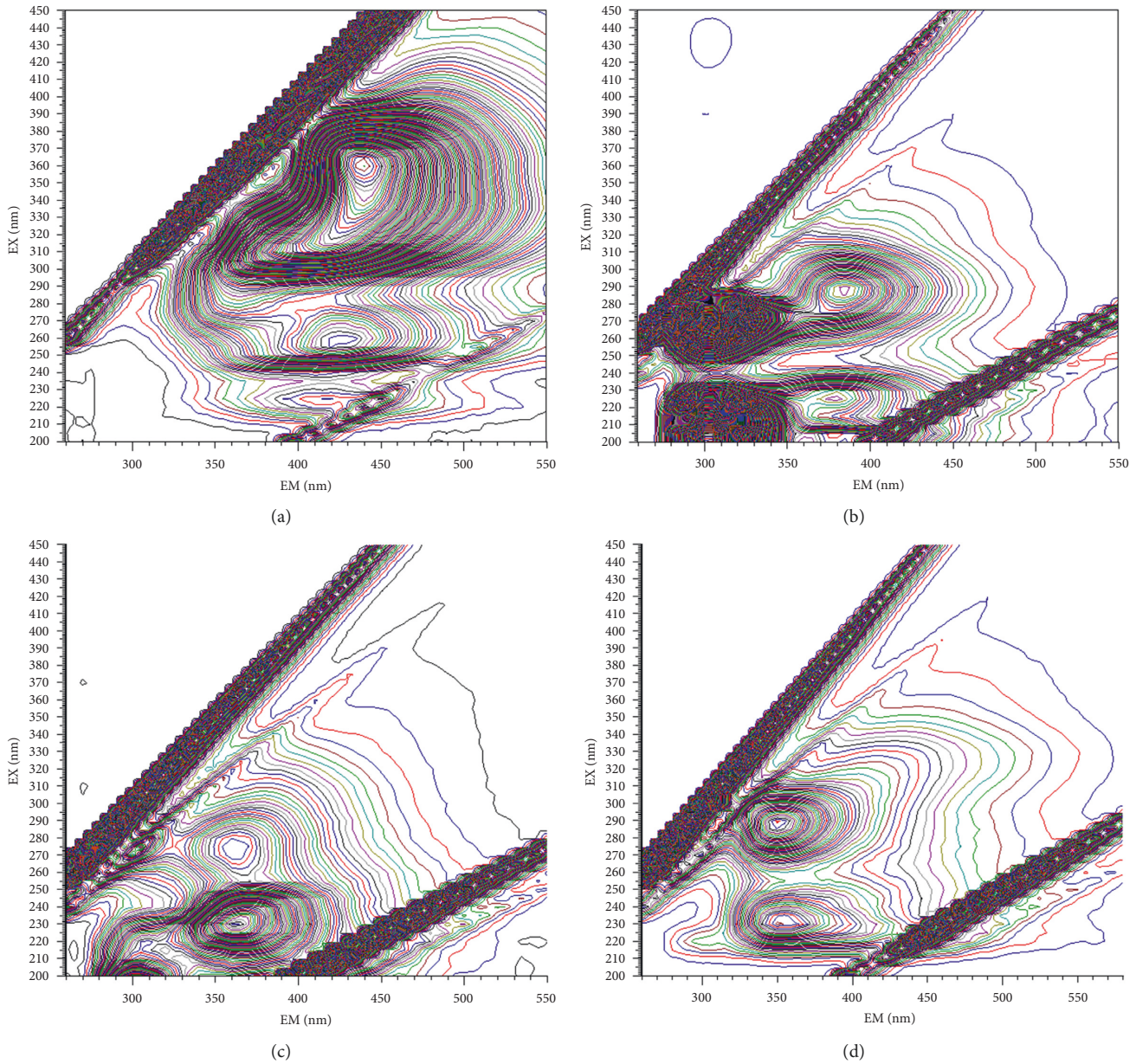


Figure 5: Continued.

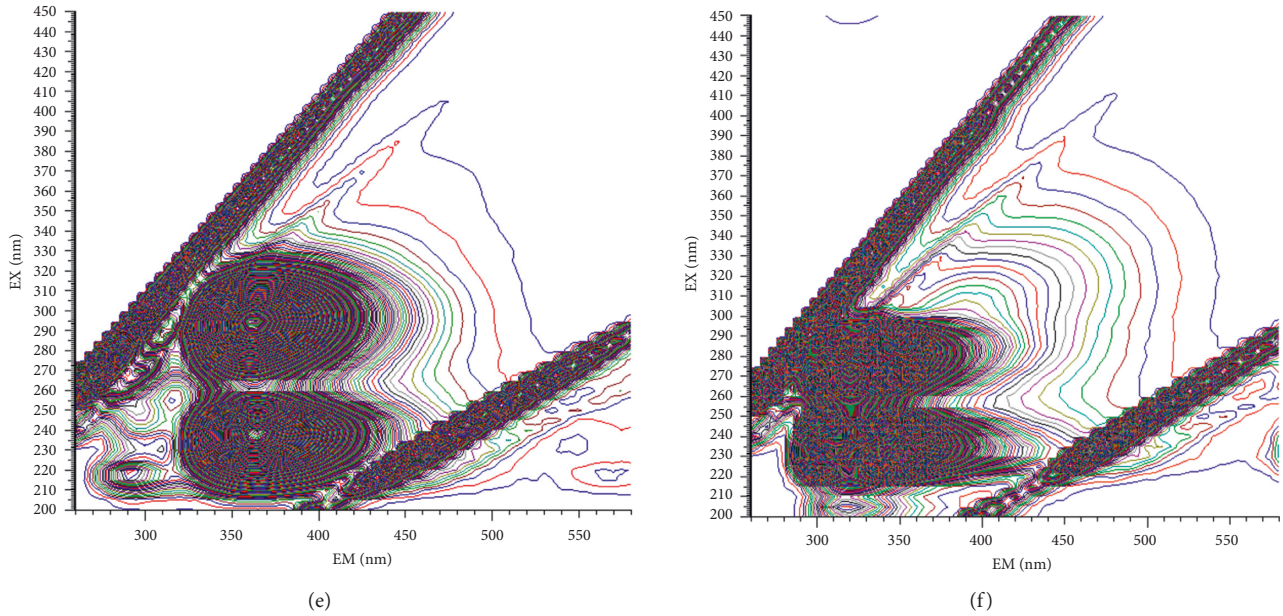


Figure 5: 3D EEM of fractions in the LCGW. (a) HoA. (b) HoB. (c) HoN. (d) HiA. (e) HiB. (f) HiN.

As shown in Table 2, the $E_{254}/E_{365}$ value of HoA increased throughout the oxidation process while that of other components decreased. This value can reflect the molecular weight, with a smaller value indicating a larger weight. The increasing $E_{254}/E_{365}$ value of HoA shows that ozone mainly reacts with macromolecular organic materials, resulting in the formation of low molecular weight organic materials. Additionally, the decreasing $E_{254}/E_{365}$ values indicate that ozone mainly reacts with low molecular weight organic materials in the HoA.

Similarly, the results indicated that the $E_{300}/E_{400}$ value of HoA was increasing throughout the oxidation process while that of other components was decreasing. The $E_{254}/E_{365}$ value can reflect the degree of humification with a lower value indicating a higher degree of humification. The HoA of untreated components had the lowest $E_{300}/E_{400}$ value, demonstrating that these samples are not suitable for biodegradation. Moreover, ozonation greatly enhanced the $E_{300}/E_{400}$ value of HoA, which is of benefit for the further biodegradation. In contrast, the $E_{300}/E_{400}$ values of other components were becoming increasingly lower, resulting in poor biodegradation.

Based on these findings, it can be inferred that, in terms of HoA, ozone mainly reacts with larger molecular recalcitrant organics to improve the performance for further degradation, while for other components, ozone degrades small organic molecules, leading to poor performance for biodegradation.

*3.4. 3D EEM for Hydrophilic and Hydrophobic Fractions before and after Ozonation.* The 3D EEM has been extensively applied to investigate the different chemical fractions of dissolved organic matter by identifying certain classes of organic matter in wastewater. The changes in 3D EEM spectra of LCGW treated by ozonation at different reaction times are shown in Figure 5. The five main regions were commonly detected in different fractions, which contain aromatic protein I, aromatic protein II, fulvic acid III, soluble microbial byproduct IV, and humic acid V. The fluorescence intensities corresponding to the peaks are shown in Table 3.

As shown in Figure 5, the hydrophobic organic compounds (HoA, HoB, and HoN) had a high degree of humification, which was probably a result of a high concentration of humic acid. However, the hydrophilic matter contained a high concentration of aromatic protein and dissolved organic matter. As a result, hydrophobic organic matter should be of more concern following ozonation. To address this issue, wastewater was bubbled with ozone to oxidize organic matter, which decreased the peak intensity. The above results were consistent with the reduction of TOC. However, the effect of ozonation occurs in two steps. In the first step, the fluorescence intensity decreased greatly after 120 min. As shown in Table 3 and Figure 6, the peak intensity of aromatic protein I decreased from 7218 to 643 and the removal rate was 91.09% in HoB. Additionally, the peak intensity of aromatic protein I decreased from 6700 to 226 and the removal rate was 96.63% in HiN. In the second step, different substances were detected in the same fractions at 120 min. Evaluation of the fluorescence at 360/440 nm revealed that the humic acid V was not present, but it was detected at 120 min in HiN. These findings indicated that parts of HoA were oxidized to HiN during the reaction, which was consistent with the results of UV-Vis and TOC analysis. Moreover, there were no changes in the types of organic materials in any of the fractions during ozonation, but all intensities of fluorescence decreased. In conclusion, during the 120 min ozonation of effluent after ammonia distillation and dephenolization, the macromolecular organics were oxidized to smaller

Table 3: Three-dimensional fluorescence spectroscopy table of DOM components.

| Time (min) | | $\lambda_{EX}/\lambda_{EM}$ (nm) | | | | | Fluorescence intensity (a.u.) | | | | |
|---|---|---|---|---|---|---|---|---|---|---|---|
| | | I | II | III | IV | V | I | II | III | IV | V |
| 0 | HoA | | | 225/420 | | 260/425 | | | 141 | | 427 |
| | | | | | | 360/440 | | | | | 1160 |
| | HoB | 215/300 | | 205/380 | 270/300 | 290/385 | 7218 | | 1058 | 5737 | 972 |
| | | | | 225/380 | | | | | 774 | | |
| | HoN | | 230/360 | | 270/360 | | | 719 | | | 346 |
| | HiA | | 230/350 | | 290/350 | | | 344 | | 523 | |
| | HiB | 220/290 | | 240/365 | 295/365 | | 227 | | 2509 | 2401 | |
| | HiN | 235/320 | | | 280/320 | | 6700 | | | 4729 | |
| 120 | HoA | | | 245/415 | | 310/410 | | | 612 | | 682 |
| | HoB | 215/315 | | 230/380 | | 300/380 | 539 | | 390 | | 340 |
| | HoN | | | | | | | | | | |
| | HiA | | | 225/400 | 270/300 | 310/405 | | | 197 | 216 | 131 |
| | HiB | 215/290 | 220/365 | | 290/370 | | 207 | 342 | | 213 | |
| | HiN | 235/320 | | 235/405 | | 315/395 | 155 | | 445 | | 581 |

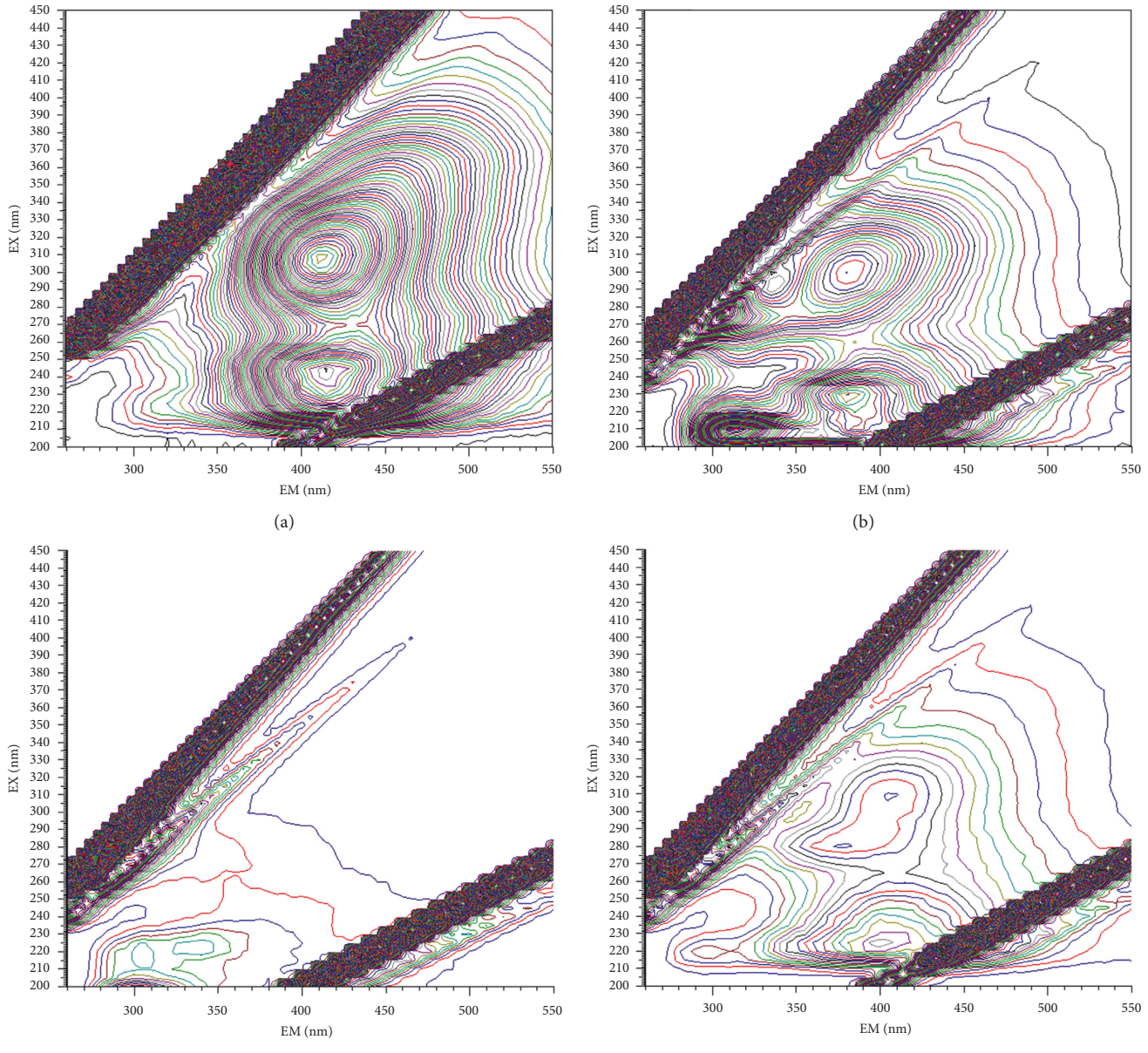


Figure 6: Continued.

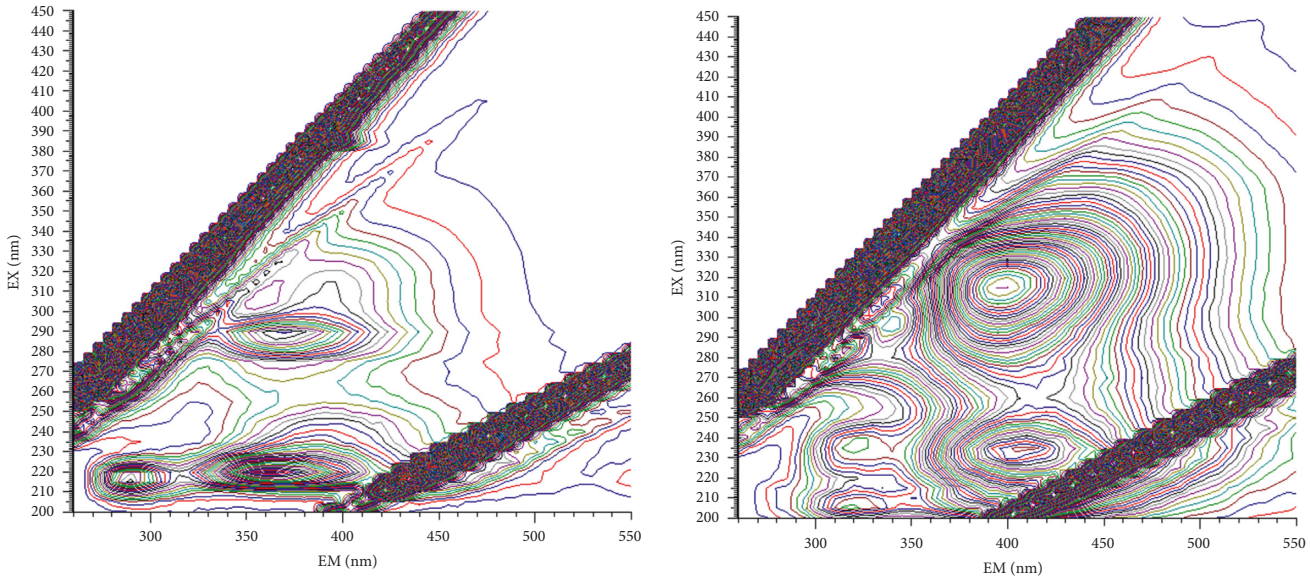


Figure 6: 3D EEM of fractions after 120 min of ozonation.(a) HoA. (b) HoB. (c) HoN. (d) HiA. (e) HiB. (f) HiN.

molecules with the degradation of soluble microbial by-products. After the organic types were changed, the residual organics were oxidized and completely removed.

## 4. Conclusions

During ozonation of effluent from ammonia distillation and dephenolization, DOM was fractionated into six classes by resin adsorption. The TOC, $UV_{254}$, UV-Vis, and 3D EEM of fractions were found to have different effects on ozonation. Additionally, the HoA and HiN fractions were found to be containing the majority TOC (about 380.21 mg·$L^{-1}$ and 646.84 mg·$L^{-1}$, resp.). Moreover, TOC removal rates of HoA and HiN reached 42.85% and 67.13%, respectively. The $UV_{254}$ values of HoA remained unchanged, while that of HiN increased continuously before and after ozonation because humic macromolecular organic materials in HoA were oxidized, and a portion of their product was HiN. Furthermore, UV-Vis analysis revealed that the HoA of ozonation primarily reacts with larger molecular recalcitrant organics to improve the performance for further degradation. The 3D EEM spectra indicated that the macromolecular organics were oxidized to smaller molecules with the degradation of soluble microbial by-products. After the organic types were changed, the residual organics were oxidized and completely removed.

## Conflicts of Interest

The authors declare that they have no conflicts of interest.

## Acknowledgments

This research was funded by the 863 Project of the Ministry of Science and Technology from China (2015AA050501).

## Supplementary Materials

Figure 1S: Relationship between ozonation effect and reaction time. Figure 2S: Influence of pH on COD removal. Figure 3S: Influence of ozone dosage on COD removal. Figure 4S: Influence of aeration on COD removal rate. (*Supplementary Materials*)

## References

[1] A. K. Singh and J. Kumar, "Fugitive methane emissions from Indian coal mining and handling activities: estimates, mitigation and opportunities for its utilization to generate clean energy," *Energy Procedia*, vol. 90, pp. 336–348, 2016.

[2] C. He, X. Feng, and K. H. Chu, "Process modeling and thermodynamic analysis of Lurgi fixed-bed coal gasifier in an SNG plant," *Applied Energy*, vol. 111, no. 11, pp. 742–757, 2013.

[3] X. Hu, K. Chen, X. Lai et al., "Treatment of pretreated coal gasification wastewater (CGW) by magnetic polyacrylic anion exchange resin," *Journal of Environmental Chemical Engineering*, vol. 4, no. 2, pp. 2040–2044, 2016.

[4] H. Gai, H. Song, M. Xiao et al., "Conceptual design of a modified phenol and ammonia recovery process for the treatment of coal gasification wastewater," *Chemical Engineering Journal*, vol. 304, pp. 621–628, 2016.

[5] S. Jia, H. Han, B. Hou et al., "Advanced treatment of biologically pretreated coal gasification wastewater by a novel integration of three-dimensional catalytic electro-Fenton and membrane bioreactor," *Bioresource Technology*, vol. 198, pp. 918–921, 2015.

[6] J. Akhlas, A. Bertucco, F. Ruggeri et al., "Treatment of wastewater from syngas wet scrubbing: model-based comparison of phenol biodegradation basin configurations," *Canadian Journal of Chemical Engineering*, vol. 95, pp. 1652–1660, 2017.

[7] H. An, Z. Liu, X. Cao et al., "Mesoporous lignite-coke as an effective adsorbent for coal gasification wastewater treatment," *Environmental Science Water Research and Technology*, vol. 3, no. 1, pp. 169–174, 2017.

[8] L. Xu, J. Wang, X. Zhang et al., "Development of a novel integrated membrane system incorporated with an activated coke adsorption unit for advanced coal gasification wastewater treatment," *Colloids and Surfaces A: Physicochemical and Engineering Aspects*, vol. 484, pp. 99–107, 2015.

[9] P. Xu, W. Ma, B. Hou et al., "A novel integration of microwave catalytic oxidation and MBBR process and its application in advanced treatment of biologically pretreated Lurgi coal gasification wastewater," *Separation and Purification Technology*, vol. 177, pp. 233–238, 2017.

[10] Z. Wang, X. Xu, Z. Gong et al., "Removal of COD, phenols and ammonium from Lurgi coal gasification wastewater using $A^2O$-MBR system," *Journal of Hazardous Materials*, vol. 235-236, pp. 78–84, 2012.

[11] Y. Li, S. Tabassum, and Z. Zhang, "An advanced anaerobic biofilter with effluent recirculation for phenol removal and methane production in treatment of coal gasification wastewater," *Journal of Environmental Sciences*, vol. 47, pp. 23–33, 2016.

[12] Y. Jeong and J. S. Chung, "Simultaneous removal of COD, thiocyanate, cyanide and nitrogen from coal process wastewater using fluidized biofilm process," *Process Biochemistry*, vol. 1, no. 41, pp. 1141–1147, 2006.

[13] Y. Li, G. Gu, J. Zhao et al., "Treatment of coke-plant wastewater by biofilm systems for removal of organic compounds and nitrogen," *Chemosphere*, vol. 52, no. 6, pp. 997–1005, 2003.

[14] F. Guan, G. Gao, and Q. Zhao, "Treatment of coal gasification wastewater by A/O biofilm process," *China Water and Wastewater*, vol. 25, pp. 74–76, 2009.

[15] H. Zhuang, S. Shan, C. Fang et al., "Advanced treatment of biologically pretreated coal gasification wastewater using a novel expansive flow biological intermittent aerated filter process with a ceramic filler from reused coal fly ash," *RSC Advances*, vol. 6, no. 46, pp. 39940–39946, 2016.

[16] Q. Liu, S. Vijay, P. Z. Fu et al., "An anoxic-aerobic system for simultaneous biodegradation of phenol and ammonia in a sequencing batch reactor," *Environmental Science and Pollution Research*, vol. 24, no. 12, pp. 11789–11799, 2017.

[17] Q. Zhao and Y. Liu, "State of the art of biological processes for coal gasification wastewater treatment," *Biotechnology Advances*, vol. 34, no. 5, pp. 1064–1072, 2016.

[18] C. Yang, Y. Qian, L. Zhang et al., "Solvent extraction process development and on-site trial-plant for phenol removal from industrial coal-gasification wastewater," *Chemical Engineering Journal*, vol. 117, no. 2, pp. 179–185, 2006.

[19] C. Lin, X. Zhuo, X. Yu et al., "Identification of disinfection by-product precursors from the discharge of a coking wastewater treatment plant," *RSC Advances*, vol. 54, no. 5, pp. 43786–43797, 2015.

[20] J. Swietlik, A. Dabrowska, and U. Raczykstanisławiak, "Reactivity of natural organic matter fractions with chlorine dioxide and ozone," *Water Research*, vol. 38, no. 3, pp. 547–558, 2004.

[21] T. Zhang, J. Liu, and J. Ma, "Comparative study of ozonation and synthetic goethite-catalyzed ozonation of individual NOM fractions isolated and fractionated from a filtered river water," *Water Research*, vol. 42, no. 6-7, pp. 1563–1570, 2008.

[22] F. Qi, W. Chu, and B. Xu, "Comparison of phenacetin degradation in aqueous solutions by catalytic ozonation with $CuFe_2O_4$, and its precursor: Surface properties, intermediates and reaction mechanisms," *Chemical Engineering Journal*, vol. 284, pp. 28–36, 2016.